Optimization of the continuous coprecipitation in a microfluidic reactor: Cu-based catalysts for CO2 hydrogenation into methanol

Valentin l'Hospital, Svetlana Heyte, Sébastien Paul, Ksenia Parkhomenko, Anne-Cécile Roger

Version of Record: https://www.sciencedirect.com/science/article/pii/S0016236122005531
Manuscript_74c7e382afb383e83c4ad6cf4255ccba

Optimization of the continuous coprecipitation in a microfluidic reactor: Cu-based catalysts for CO_2 hydrogenation into methanol

Valentin L'hospital[a], Svetlana Heyte[b], Sébastien Paul[b], Ksenia Parkhomenko[a], Anne-Cécile Roger[a,*]

[a] ICPEES, Équipe "Énergie et Carburants pour un Environnement Durable" UMR CNRS 7515, ECPM, Université de Strasbourg, 25 rue Becquerel, 67087 Strasbourg Cedex 2, France

[b] Univ. Lille, CNRS, Centrale Lille, Univ. Artois, UMR 8181, UCCS, Unité de Catalyse et Chimie du Solide, F-59000 Lille, France

GRAPHICAL ABSTRACT

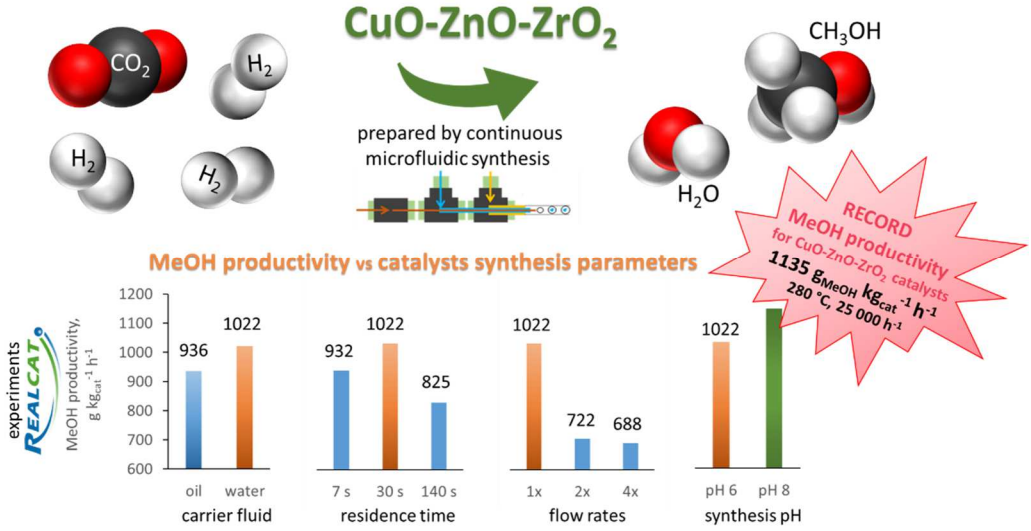

ABSTRACT

CuO-ZnO-ZrO_2 catalysts were synthetized by controlled continuous coprecipitation in a microfluidic reactor. CuO, ZnO and ZrO_2 contents in catalysts were kept constant at 37.5 wt% of CuO (corresponding to 30% Cu^0), 41.0 wt% of ZnO and 21.5 wt% of ZrO_2. Numerous parameters of the continuous microfluidic coprecipitation, such as the nature of the carrier fluid, the residence time in the microfluidic synthesis reactor, the reagents flow rates during the synthesis and the pH, were studied in order to obtain perfectly homogeneous catalytic materials. All catalysts were characterized and then tested in methanol synthesis via CO_2 hydrogenation on the REALCAT platform using high-throughput experiments. The optimum catalytic results were obtained for the catalyst synthesized by the continuous coprecipitation in a microfluidic reactor at following controlled parameters: water as carrier fluid, 30 s of residence time, low total reagent flowrate of 35 µL $min^{-1}$and pH equal to 8. This catalyst presented a good CO_2 conversion of 21.4 % along with a methanol selectivity of 33 %, leading to a record methanol productivity of 1135 g_{MeOH} kg_{cat}^{-1} h^{-1} at 280 °C, 50 bar and a GHSV of 25,000 h^{-1} (STP).

Highlights

- CuO-ZnO-ZrO_2 catalysts were prepared via continuous coprecipitation in a microfluidic reactor.
- High-throughput catalytic tests were carried out on the REALCAT platform.
- The optimized catalyst showed a record methanol productivity of 1135 g_{MeOH} kg_{cat}^{-1} h^{-1} at 280 °C, 50 bar and 25,000 h^{-1}.

- Optimized parameters for the microfluidic catalyst preparation: water as vector fluid, residence time 30 s, low reagents flow rate and precipitation pH = 8.

Keywords

methanol synthesis, CuO-ZnO-ZrO_2 catalyst, continuous coprecipitation, microfluidic reactor, high-throughput experiments

1. Introduction

Anthropogenic Green House Gases (GHG) emissions coming from industrial development and from the use of fossil fuels as coal, oil and natural gas have risen sharply during last decades. Fossil fuels are strong emitters of GHG, especially CO_2, which is one of GHG the most impacting the climate change [1]. The abatement of CO_2 emissions is already on the road by capture and storage. One of the most promising solutions stays the CO_2 direct transformation to chemicals, such as urea [2], salicylic acid [3], or polycarbonates [4]. However, these chemicals have a limited size of the markets, so other solutions must be developed in order to reuse the CO_2 as a carbon source for efficient storage in chemical intermediates or energy vector molecules, as methanol [5-7]. It is a very important chemical intermediate produced in large quantities, up to 80 Mt in 2016 [8] and widely used for the production of formaldehyde [9], dimethyl ether [10], polymer precursors such as ethylene and propylene [11,12] as well as methyl tert-butyl ether (MTBE) [13]. In general, methanol formation from CO_2 is considered as a key process in the Power-to-X technologies: firstly methanol is synthesized in a reactor by use of renewable energy sources[14]. Secondly it can be upgraded to fuels (gasoline, diesel, kerosene, olefins, and ethers) through several additional chemical processes (additional reactors, separation unit, purification unit, distillation unit, flash unit, and absorber) to be used in the transportation and other commercial applications[15].

Nowadays, methanol is produced via the reaction CO hydrogenation in presence of a metal catalyst [16]. In the 1960s, a new catalyst - copper oxide dispersed over zinc oxide - was developed and used at temperatures of 250-350 °C and pressures of 50-100 bar [17]. Then, these catalysts were modified adding alumina (Al_2O_3) support. Until now this type of catalyst is still used to convert H_2/CO_2 mixtures with or without CO to methanol [18-24]. The use of pure CO_2 and not CO/CO_2 forced to the addition of zirconia (ZrO_2) with its basic character in the support that allowed to increase the dispersion of copper and zinc oxide by decreasing the crystallite size and increasing the specific surface area [25]. Zirconia plays a role in the reaction mechanism by participating in CO_2 adsorption [26,27]. Sintering of copper and ZnO could be also decreased in the presence of zirconia [25]. Koeppel *et al.* [28] have described the improved formation of methanol due to the Cu-ZrO_2 interface, as microcrystalline copper particles are stabilized by an amorphous ZrO_2 matrix. Their work shows that H_2 is adsorbed on metallic copper and CO_2 is adsorbed on ZnO and ZrO_2 in close vicinity with the metal sites, allowing the hydrogenation of the intermediate formates [29]. To promote this intimate interaction between the three species and improve more the hydrogenation reaction the fine control of the preparation of the catalyst should be done. The methanol synthesis from CO_2 (eq. 1) is always in competition with the reverse water-gas shift reaction (RWGS) (eq. 2). The addition of ZrO_2 in the catalyst composition replacing Al_2O_3 was found to create an activity gap, may suppress the CO selectivity and improves the selectivity of methanol formation.[30] It was also suggested that the surface Lewis acid Zr(IV) sites close to Cu metallic sites are responsible for the enhanced performances of the Cu/ZrO_2-based catalysts.[31]

$CO_2 + 3H_2 \leftrightarrows CH_3OH + H_2O$ $\Delta_rH°_{25°C} = -49.8$ kJ.mol^{-1} *eq. (1)*

$CO_2 + H_2 \leftrightarrows CO + H_2O$ $\Delta_rH°_{25°C} = 41.0$ kJ.mol^{-1} *eq. (2)*

One of the simplest method of solid composite catalysts' preparation is the coprecipitation method. Several metal cations precipitate together in the form of well-mixed carbonates, hydroxides or hydroxycarbonates, preserving in the solid state the perfect mixture of cations induced by their initial dissolution in a solvent. Usually Na_2CO_3, $(NH_4)_2CO_3$ or NaOH are used as precipitating agents.[32-34] The coprecipitation method of catalysts' synthesis promotes an intimate mixture of the metal cations at the atomic level thus allowing a good interaction between them in the final catalytic material [19]. Nevertheless, many parameters of the coprecipitation synthesis may strongly influence the homogeneity of the final material as the pH and the temperature[35,36], the aging time [29,35] and the washing step of the precipitate. Even if all the parameters are carefully controlled in batch or continuous classical coprecipitation synthesis, heterogeneous zones will arise due to concentration gradients or unideal mixing.

For the first time a preparation method of the continuous coprecipitation synthesis to overcome the problems of heterogeneity of the final catalytic materials was presented in our previous work [37]. This method was inspired by the use of micromixers [38], microemulsions [39] and microreactors [40]. The continuous coprecipitation process is based on the formation of droplets formed by reagents brought by a carrier fluid. The droplets are more precisely formed by the mixture of two starting aqueous solutions of the metal cations and of the precipitating agent [41,42]. Upon the mixture of these solutions, coprecipitation occurs in a very small volume of one droplet size, allowing to reproduce the same environment and the same conditions for each droplet. It was shown that the CuO-ZnO-ZrO_2 catalyst with the same composition prepared by this new method presented superior methanol productivity compared to the one prepared by the coprecipitation at constant pH [37]. The novel synthesis method allowed a better repeatability and homogeneity of the catalyst leading to the methanol productivity of 486 $g_{MeOH}\ kg_{cata}^{-1}\ h^{-1}$ at 280 °C under 50 bar and a GHSV of 10,000 h^{-1}. This result was then improved by adjusting the catalyst composition, the ratio ZnO/ZrO_2 was varied. The optimum catalytic results were obtained for the 30Cu-$ZZ_{66/34}$ catalyst whose support was composed of 66 wt% of ZnO and 34 wt% of ZrO_2. This catalyst presented CO_2 conversion 19.6 % and methanol selectivity 50 %, leading to a methanol productivity of 725 $g_{MeOH}\ kg_{Cata}^{-1}\ h^{-1}$ at 280 °C, 50 bar and a GHSV of 25,000 h^{-1} (STP). In the literature, one of the best productivities in methanol over Cu-Zn-Zr catalyst was presented by Saito *et al.*[43] with a 50Cu-Zn-Zr catalyst, a methanol productivity of 620 $g_{MeOH}\ kg_{cat}^{-1}\ h^{-1}$ was obtained in the similar conditions (250°C, 18 000 L h^{-1}, H_2/CO_2=3). Bonura *et al.*[27] indicated that their 60Cu-Zn-Zr catalyst led to a methanol productivity about 305 $g_{MeOH}\ kg_{cat}^{-1}\ h^{-1}$ with a higher copper content, the reaction was performed at 30 bar and 240 °C and 10,000 h^{-1}. More recently, in the work of Witoon *et al.*[44], a methanol productivity of 274 $g_{MeOH}\ kg_{cat}^{-1}\ h^{-1}$ at 240 °C and 20 bar has been obtained.

Even though in our previous work the Zn/Zr ratio in the catalyst composition was optimized, the operating parameters of the synthesis in a microfluidic reactor were never changed. It is essential to optimize the synthesis parameters in order to improve the catalysts. In this study, the CuO-ZnO-ZrO_2 (CZZ) material with an optimal Zn/Zr ratio [45] was chosen as catalyst for methanol synthesis from CO_2 hydrogenation. The chemical composition was following 37.5 wt% of CuO (corresponding to 30% Cu^0), 41.0 wt% of ZnO and 21.5 wt% of ZrO_2. The novelty of the present work is the deep study and the optimisation of the continuous

coprecipitation synthesis parameters. This study will help to understand the influence of each parameter at the droplet scale where coprecipitation takes place. Thus, the effects of changing conditions will be clearly evidenced thanks to controlled synthesis parameters that allow obtaining very homogeneous materials. The following parameters have been modified: the nature of the carrier fluid necessary for droplets formation, the residence time of the precipitate in the microfluidic synthesis reactor, the reagents flow rates during the synthesis and the pH of the coprecipitation. Hereafter, the influence of these parameters on the materials properties and on the catalytic results in the CO_2 hydrogenation into methanol will be described.

2. Experimental

2.1. Catalyst preparation

CuO-ZnO-ZrO_2 catalysts (CZZ) were synthesized by a continuous coprecipitation in the microfluidic reactor. All catalysts contain 37.5 % by weight of CuO (corresponding to 30 % Cu^0), 41 wt % of ZnO and 21.5 wt % of ZrO_2 (mass ratio ZnO/ZrO_2 = 66/34).[45] Schematically the microfluidic system is presented in Supplementary Information, *Figure S1*. The coprecipitation is taking place at the exit of the microfluidic reactor (*Figure 1*) in the continuously formed little droplets of diameter around 700 µm, made by the mixture of two solutions of metal cations (11.6 µL min^{-1}, 1.0 M, nitrate salts $Cu(NO_3)_2.3H_2O$ and $Zn(NO_3)_2.6H_2O$ and zirconium oxynitrate $ZrO(NO_3)_2.6H_2O$) and of the precipitating agent (23.4 µL min^{-1}, 1.6 M, Na_2CO_3). The flowrate of silicon oil (1.7 mL min^{-1}, kinematic viscosity of 5.0 m^2 s^{-1}) or water with controlled pH (6.0 or 8.0) as the carrier fluid is kept constant. The media pH was always kept stable due to the pH adjustment with HNO_3 or NaOH of the initial solutions. The carbonates/metals molar ratio was fixed at 3.5. The precipitate was aged for one night in the mother liquor, at 60-65 °C and then filtered, washed with petroleum ether to remove the silicon oil and dried for 48 h at 100 °C. The resulting powders were then calcined in air at 400 °C, with a heating ramp of 2 °C min^{-1}, for 4 h to give fresh CZZ catalysts.

The notation is exemplified as follows: $CZZ_{a\text{-}b\text{-}c\text{-}d}$ refers to a catalyst where a = vector fluid, b = residence time, c = flow rate reagent multiplication, the initial flow rate of reagent is 35 µL min^{-1} (annotated as "1x"), 70 µL min^{-1} for the "2x" flow rate and 140 µL min^{-1} for the "4x" flow rate, d = precipitation pH, corresponds to the modification of parameters during the synthesis (oil or water as carrier fluid; 7 s, 30 s or 140 s as residence time in the microfluidic synthesis reactor; 1x, 2x or 4x as multiplication of the reagent flowrates during the synthesis; pH6 or pH8 as the actual pH of coprecipitation). Example of the catalyst $CZZ_{water\text{-}30s\text{-}1x\text{-}pH6}$ corresponds to the use of water as a vector fluid, residence time was 30 s, flow multiplication was equal to 1 and pH of the catalyst synthesis was equal to 6.

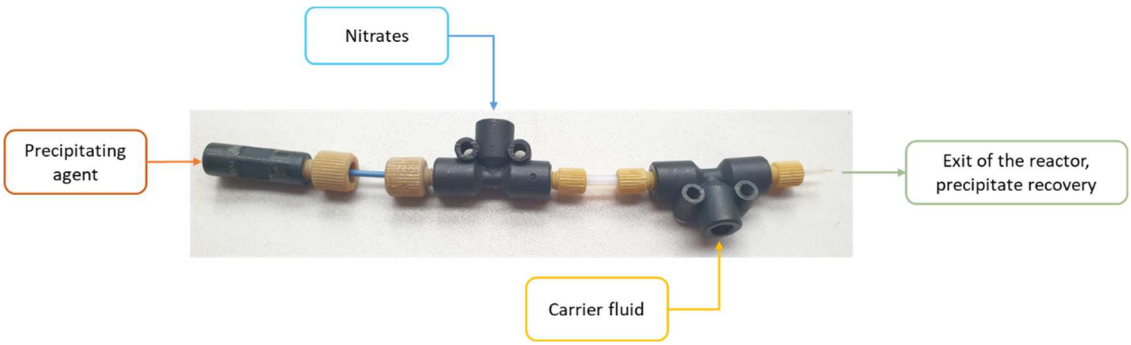

Figure 1 Microfluidic reactor for the catalysts preparation.

2.2. Catalyst characterization

Specific surface area measurements were performed by nitrogen adsorption-desorption at –196 °C using the Brunauer-Emmet-Teller (BET) method on a Micromeritics ASAP 2420 apparatus. Samples were previously outgassed at 250 °C overnight to remove the adsorbed moisture.

Reducibility studies were performed by temperature-programmed reduction (TPR-H_2) on a Micromeritics AutoChem II 2920 with 50 mg of fresh catalyst and a total flow rate of 50 mL min^{-1} of 10 % H_2 in Ar with a heating ramp of 10 °C min^{-1} until 500 °C.

The copper metallic surface area was determined by N_2O surface reaction on a Micromeritics AutoChem II 2920 apparatus [46]. Firstly, approximately 500 mg of fresh catalyst were reduced at 300 °C, heating rate 1 °C min^{-1}, hold time 12 h, under a flow of 50 mL min^{-1} of 10 % H_2 in Ar. Then the reduced catalyst was purged with Ar and cooled down to 50 °C followed by the treatment of 50 mL min^{-1} of 2 % N_2O in Ar for 15 min, the N_2O consumption was registered by TCD detector. The metallic surface area was calculated by quantifying the amount of consumed N_2O and assumption of 1.46 10^{19} copper atoms per square meter [47].

The crystalline structure of the catalysts was determined by X-ray diffraction (XRD) with a Bruker D8 Advance diffractometer equipped with a LYNXEYE detector and a Ni filter for CuK_α radiations over a 2θ range between 10 and 95 ° and a step of 0.016 ° every 0.5 s. The crystallite size was calculated using the Debye-Scherrer equation.[48]

The morphology of the catalysts was studied with a ZEISS GEMINI SEM 500 scanning electron microscope (SEM) with a resolution of 1.2 nm at 500 V and 1.1 nm at 1 kV, equipped with an Inlens secondary electron (SE) detector and a SE2 detector.

The TEM analyzes were made with a transmission electron microscope JEOL 2100, equipped with a LaB_6 filament and a High Resolution (HR) polar part allowing a point-to-point resolution of 0.2 nm to 200 kV (voltage) maximum equipped with an X-ray detector (EDX energy dispersive X-ray spectrometry) of the SDD (Silicon drift detector) type.

The elemental analysis was done by ICP-OES with a 720-ES ICP-OES equipment (Agilent). The sample (10 mg) was dissolved in hydrofluoric acid (1.5 mL), heated at 80 °C during 4 h. Then aqua regia (2.4 mL) was added and the mixture was heated during 2 h at 80 °C. After that, each sample dissolved as described above was submitted to ultrasound treatment stirred overnight in a hot water bath (50 °C). Prior to the analysis 50 mL of ultrapure water was added.

2.3. Catalytic activity

The catalytic performances were evaluated on the high-throughput catalytic screening platform named REALCAT, located in Lille, France. The 16 isothermal fixed-bed reactors of a Flowrence unit from Avantium were used simultaneously (Supplementary Information, *Figure S2*). The reactors are stainless steel tubes with an internal diameter of 2.0 mm and 15 cm long (see the scheme of the reactor in Supplementary Information, *Figure S3*). The layer of the catalytic bed in each test was kept constant at 2.8 cm, for this reason the catalyst was diluted in SiC (50-150 µm). The total flow 282 mL min^{-1} (STP) was equally divided into the 16 reactors. The gas phase molar composition was $H_2/CO_2/He$ = 3.9/1.0/0.7, this ratio was

chosen in order to compare the results with previous work.[35,43] The GHSV in each reactor was set at 25,000 h^{-1} (STP) thus the catalysts loading was adjusted depending on the apparent density of each sample. For one sample a comparison was done also at different GHSV: 10,000 and 39,000 h^{-1} (STP). In general, the GHSV (h^{-1}) was calculated according to the following equation (SiC is not taken into account for calculation):

$$GHSV\ (h^{-1}) = \frac{Q_{total} \times d_{app_{Cat}}}{m_{Cat}},$$

Where Q_{total}, the total reactant flowrate ($cm^3\ h^{-1}$), $d_{app_{Cat}}$ the apparent density of the catalyst ($g\ cm^{-3}$) and m_{Cat} the catalyst mass (g).

The unit was equipped with an online Agilent 7890 Gas Chromatograph equipped with two TCD (PPQ and HayeSepQ/Molecular Sieve columns) and one FID (CP-Sil5 column) detectors. The effluents of each reactor were analysed successively one after the other.
Prior to each test, the catalysts were reduced for 12 h under a constant flow of H_2 of 160 $mL.min^{-1}$ (STP) for the 16 reactors at 300 °C (heating rate 1 $°C.min^{-1}$), i.e. 10 mL min^{-1} (STP) of H_2 per reactor. After the reduction the system was cooled down to 150 °C and purged with the reaction mixture gas until stabilization in order to analyse the composition of the gases before the reaction. The pressure was increased till 50 bar. Then the temperature was increased by 1 $°C.min^{-1}$ to reach 200 °C, which corresponds to the first tested reaction temperature, after 30 min stabilization time the outgas of each reactor was analysed. Then the reaction temperature was progressively increased by 20 °C steps for different reaction temperatures screening until 320 °C.

The CO_2 and H_2 conversion (X_{CO2} and X_{H2}) were determined by comparing the flow rates at a time t (CO_2 or H_2) compared to the average flow of the blank achieved at 150 °C. The selectivities (S_{CO} and S_{MeOH}) were calculated from the ratio of the flow rate (CO or MeOH) to the flow rate of CO_2 consumed at the same time t.

The methanol productivity (P_{MeOH}) was calculated per mass of catalyst ($g_{MeOH}\ kg_{cat}^{-1}\ h^{-1}$) using the following equation:

$$P_{MeOH} = \frac{m_{MeOH(liquid+gas)}}{m_{Cat} \times t}$$

Where $m_{MeOH(liquid+gas)}$, the mass of methanol in the liquid and gas phase obtained during the reaction (g), m_{cat} the catalyst mass (kg) and t, the time of the reaction (h).

Then, the TOF_{MeOH} (Turnover frequency for MeOH formation) (s^{-1}) was calculated according to the following equation:

$$TOF_{MeOH} = \frac{P_{MeOH} \times N_A}{M_{MeOH} \times N_S \times S_{Cu°}}$$

Where N_A, the Avogadro Number ($6.022\ 10^{23}\ mol^{-1}$), M_{MeOH} the methanol molar mass ($g\ mol^{-1}$) and $S_{Cu°}$, the metallic copper surface area ($m^2\ g^{-1}$).

The thermodynamic calculations were made using the ProSimPlus3 software with a Soave-Redlich-Kwong equation of state. A Gibbs reactor was used, based on the minimization of the Gibbs energy of the defined thermodynamic system (CO_2, H_2, CH_3OH, H_2O and CO).

3. Results and discussion

The continuous coprecipitation in a microfluidic system was firstly carried out using silicon oil and water for comparison. Secondly, the conditions of the continuous coprecipitation in a microfluidic reactor were optimized.

3.1. Continuous coprecipitation in a microfluidic reactor: water vs silicon oil

Table 1 summarizes the different characterization results obtained for two materials prepared using different carrier fluids (silicon oil or water): $CZZ_{oil\text{-}30s\text{-}1x\text{-}pH6}$ and $CZZ_{water\text{-}30s\text{-}1x\text{-}pH6}$. All the other conditions of preparation were the same.

Table 1 Characterization of CZZ catalysts with different carrier fluids

Catalysts	Elementary analysis (wt %) #			$d_{app_{cat}}$ $ (g cm^{-3})	Crystallite size (nm)¤		S_{BET} ($m^2 g^{-1}$)	S_{Cu° ($m_{Cu^\circ}{}^2 g_{cat}^{-1}$)
	CuO (37.5)*	ZnO (41.0)*	ZrO_2 (21.5)*		CuO	ZnO		
$CZZ_{oil\text{-}30s\text{-}1x\text{-}pH6}$	43	29	28	0.49	12	13	87	9.2
$CZZ_{water\text{-}30s\text{-}1x\text{-}pH6}$	40	38	22	0.42	10	11	99	9.4

$CZZ_{a\text{-}b\text{-}c\text{-}d}$: a = vector fluid, b = residence time, c = flow multiplication, d = precipitation pH
$ apparent density of the catalyst
 # determined by ICP-OES
*** theoretical values**
¤ determine by XRD with Debye-Scherrer equation

Using the silicon oil as a carrier fluid, the chemical composition of $CZZ_{oil\text{-}30s\text{-}1x\text{-}pH6}$ slightly differs from the theoretical composition. In particular, the ZnO content is much smaller than expected. It seems that using this kind of carrier fluid, the precipitation of Zn cations is not complete. The apparent density is slightly higher for the catalyst synthesized with oil as carrier fluid. Regarding the specific surface areas, the material synthesized using the silicon oil has smaller BET surface area (87 $m^2 g^{-1}$ for $CZZ_{oil\text{-}30s\text{-}1x\text{-}pH6}$ vs 99 $m^2 g^{-1}$ for $CZZ_{water\text{-}30s\text{-}1x\text{-}pH6}$), its porosity is estimated smaller as well and thus the catalytic bed is denser than that of the material prepared using water as carrier fluid (apparent density 0.49 vs 0.42, respectively). The carrier fluid does not influence the metallic copper surface area, the two values being quite close (9.2 and 9.4 $m_{Cu^\circ}{}^2 g^{-1}$). *Figure 2* shows the H_2-TPR profiles of H_2 consumption for both catalysts $CZZ_{oil\text{-}30s\text{-}1x\text{-}pH6}$ and $CZZ_{water\text{-}30s\text{-}1x\text{-}pH6}$. It seems that the carrier fluid nature has an influence on the copper reduction temperature. When the silicon oil is used, the main reduction temperature peak is quite smooth and its maximum is at 226 °C comparing to 215 °C when water is used as the carrier fluid. Additionally, $CZZ_{water\text{-}30s\text{-}1x\text{-}pH6}$ material shows the presence of 2 shoulders on the main peak before and after 215 °C. This could mean that copper is present in several forms interacting with the support, assuming that the accessibility of copper on the surface is easier when water is used as a carrier fluid, and the CuO-support interaction is slightly stronger for $CZZ_{oil\text{-}30s\text{-}1x\text{-}pH6}$. The possible reason of the multispecies reduction profile is coming out from XRD results of the dried precursors before calcination (XRD profiles are provided in Supplementary Information, *Figure S4*). Actually two phases, aurichalcite and malachite, are formed in the case of the synthesis in water, and only one phase aurichalcite is formed when oil is used as a carrier fluid.

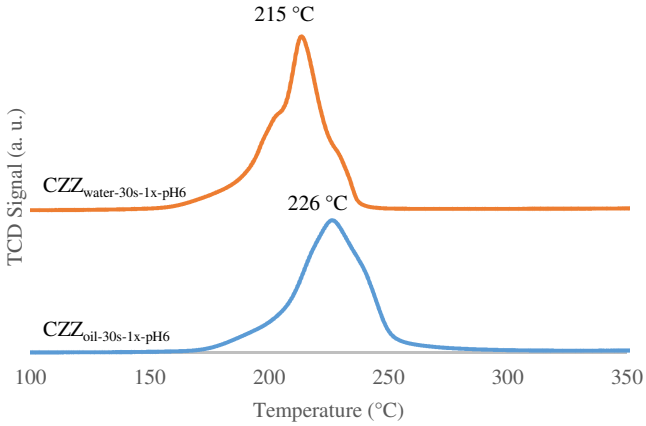

Figure 2 TPR-H_2 profiles of $CZZ_{oil\text{-}30s\text{-}1x\text{-}pH6}$ and $CZZ_{water\text{-}30s\text{-}1x\text{-}pH6}$ catalysts

Figure 3 shows scanning electron microscopy (SEM) images of CZZ_{oil}-30s-1x-pH6 and CZZ_{water}-30s-1x-pH6 catalysts. The morphology of the CZZ_{oil}-30s-1x-pH6 catalyst is more compact and granular compared to the fine and porous layered morphology for CZZ_{water}-30s-1x-pH6. This explains the higher specific BET surface and the lower apparent density for CZZ_{water}-30s-1x-pH6. It would therefore seem that by changing the carrier fluid, the morphology could be changed and a layered flower-like structure could be formed using water.

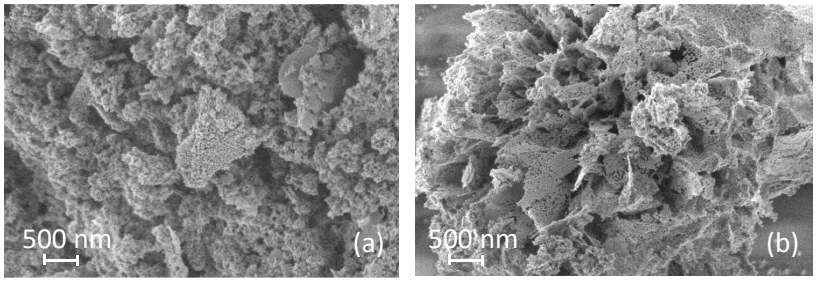

Figure 1 SEM images of (a) $CZZ_{oil\text{-}30s\text{-}1x\text{-}pH6}$ and (b) $CZZ_{water\text{-}30s\text{-}1x\text{-}pH6}$

Both catalysts were analysed by transmission electron microscopy (TEM), the images are shown in *Figure 4*. The images (a) and (b) correspond to CZZ_{oil}-30s-1x-pH6, the images (c) and (d) correspond to CZZ_{water}-30s-1x-pH6. The image 4(a) shows two distinct zones composed of different crystallite sizes: zone A (purple) granular with small crystal sizes (7 to 10 nm) and zone B (blue) with larger crystals (25 to 40 nm). The image 4(b) shows the presence of a crystallized zone (yellow, visible moiré effect is due to crystal planes overlapping) and another amorphous zone (green). The structure of the CZZ_{water}-30s-1x-pH6 presented in the images 4(c) and 4(d) is much more homogeneous with probably an improved interaction between copper, zinc and zirconium oxides. The average size of the crystals is between 13 and 25 nm, which is twice smaller than in case of CZZ_{oil}-30s-1x-pH6.

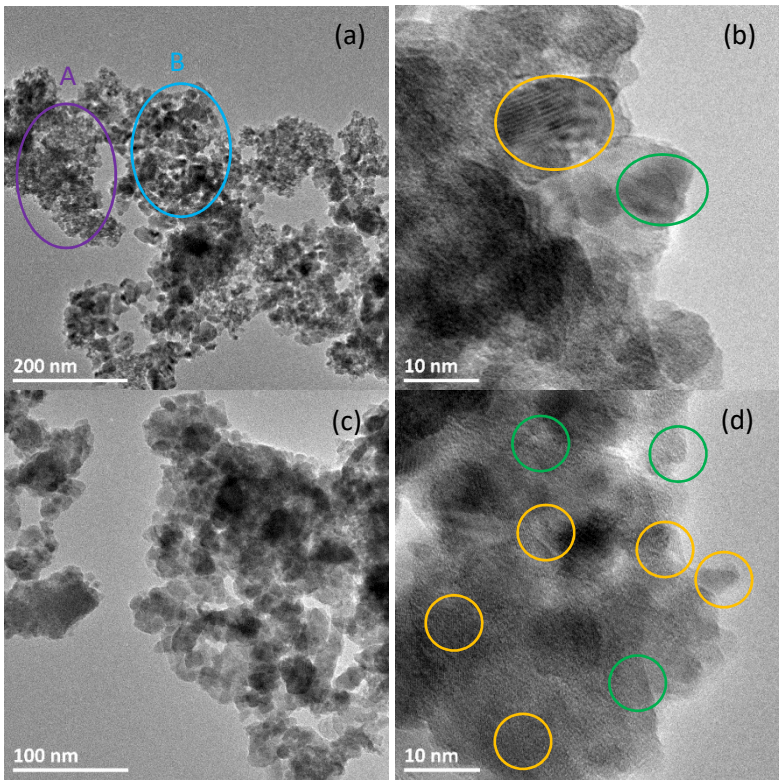

Figure 4 Bright field TEM images of (a, b) $CZZ_{oil\text{-}30s\text{-}1x\text{-}pH6}$ and of (c, d) $CZZ_{water\text{-}30s\text{-}1x\text{-}pH6}$

The catalytic results of the CO_2 hydrogenation into methanol between 200 and 320 °C at 50 bar with a GHSV of 25,000 h^{-1} as well as the thermodynamic equilibrium values are presented in *Table 2*. The same results presented in the form of a diagram are shown in Supplementary Information, *Figure S5*. The catalytic activity was stable at low temperatures and a small deactivation slope appears at high temperatures (more than 300 °C). The graph with the results of catalysts' stability study is shown in Supplementary Information, *Figure S6*. In general, the influence of the reaction temperature on catalytic activity was studied for both catalysts prepared with water and oil as carrier fluid. The catalytic results for $CZZ_{oil\text{-}30s\text{-}1x\text{-}pH6}$ as well as for $CZZ_{water\text{-}30s\text{-}1x\text{-}pH6}$ indicate that the conversions of H_2 and CO_2 increase gradually with the reaction temperature until 280 °C when the H_2 conversions stabilize around 10 % whereas the CO_2 conversions keep increasing from 20 % at 280 °C to 29 % at 320 °C. These results are directly correlated with a progressive decrease in methanol selectivity in favour of carbon monoxide selectivity. The reach of the thermodynamic equilibrium at high temperature favours the Reverse Water Gas Shift (RWGS, $CO_2 + H_2 \leftrightarrows CO + H_2O$). The stabilization of H_2 conversion is directly related to these selectivity changes due to different H_2/CO_2 stoichiometry depending of these two competitive reactions: methanol synthesis and RWGS. Experimentally these phenomena are shown in *Figure 5*. The H_2 and CO_2 conversions increase with temperature and reach thermodynamic limits. The selectivity of methanol formation (*Figure 5c*) at different temperatures follows the thermodynamic predictions as well as the selectivity of CO formation (*Figure 5d*).

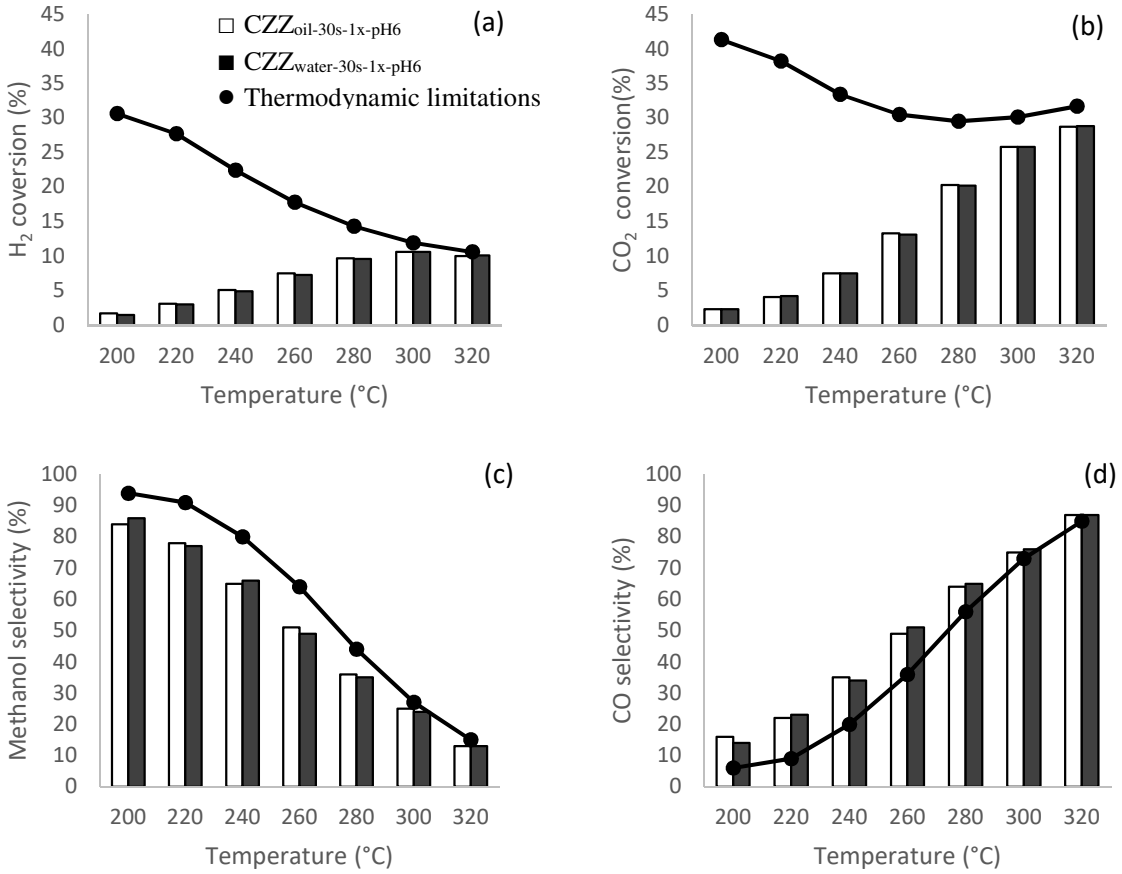

Figure 5 H_2 conversion (a); CO_2 conversion (b), MeOH selectivity (c) and CO selectivity (d) in the presence of $CZZ_{oil\text{-}30s\text{-}1x\text{-}pH6}$ (white) and $CZZ_{water\text{-}30s\text{-}1x\text{-}pH6}$ (black) catalysts, at 50 bar and 25,000 h^{-1}

Table 2 Catalytic results at 50 bar and 25,000 h^{-1} for CZZ catalysts with different carrier fluids

Catalysts (mass[#])	Temperature (°C)	Conversion (%)		Selectivity (%)		MeOH productivity (g kg_{cat}^{-1} h^{-1})	TOF (10^3 s^{-1})
		H_2	CO_2	MeOH	CO		
$CZZ_{oil\text{-}30s\text{-}1x\text{-}pH6}$ (20.1 mg)	200	1.7	2.3	84	16	249	9.7
	220	3.1	4.1	78	22	439	17.1
	240	5.1	7.5	65	35	628	24.4
	260	7.5	13.3	51	49	831	32.3
	280	**9.7**	**20.3**	**36**	**64**	**936**	**36.4**
	300	10.6	25.8	25	75	839	32.7
	320	10	28.7	13	87	481	18.7
$CZZ_{water\text{-}30s\text{-}1x\text{-}pH6}$ (17.9 mg)	200	1.5	2.3	86	14	274	10.4
	220	3.0	4.2	77	23	452	17.2
	240	4.9	7.5	66	34	680	25.9
	260	7.3	13.1	49	51	901	34.3
	280	**9.6**	**20.2**	**35**	**65**	**1022**	**38.9**
	300	10.6	25.8	24	76	876	33.4
	320	10.1	28.8	13	87	569	21.7
Thermodynamic simulation results	200	30.6	41.3	94	6	/	/
	220	27.7	38.2	91	9	/	/
	240	22.4	33.4	80	20	/	/
	260	17.8	30.5	64	36	/	/
	280	**14.3**	**29.5**	**44**	**56**	/	/
	300	11.9	30.1	27	73	/	/
	320	10.6	31.7	15	85	/	/

$CZZ_{a\text{-}b\text{-}c\text{-}d}$: a = vector fluid, b = residence time (s) , c = flow multiplication, d = precipitation pH
[#] calculated from the apparent density of each catalyst in keep constant GHSV

The best methanol productivity for both samples was obtained at 280 °C: 936 g_{MeOH} kg_{cat}^{-1} h^{-1} for $CZZ_{oil\text{-}30s\text{-}1x\text{-}pH6}$ and 1022 g_{MeOH} kg_{cat}^{-1} h^{-1} for $CZZ_{water\text{-}30s\text{-}1x\text{-}pH6}$. The reaction parameters as hydrogen and CO_2 conversion as well as methanol and CO selectivities were very close for both catalysts (Table 2). Regarding the difference in morphology, smaller specific surface area and slightly denser $CZZ_{oil\text{-}30s\text{-}1x\text{-}pH6}$ material, the productivity in methanol recalculated as TOF shows the beneficial use of water as the carrier fluid in the microfluidic reactor system during the catalytic materials synthesis. Indeed, the catalyst $CZZ_{water\text{-}30s\text{-}1x\text{-}pH6}$ has a better homogeneity between the various oxides, porous and light layered flower-like morphology, that allowed a record performance in CO_2 hydrogenation to methanol in terms of methanol productivity (1022 g_{MeOH} kg_{cat}^{-1} h^{-1} at 280 °C, 50 bar, GHSV 25,000 h^{-1}). Additionally, the use of silicon oil as the carrier fluid for scaled-up production would bring some ecological concerns. For these reasons, water was chosen as the carrier fluid further studies and other parameters were optimized.

3.2. Continuous coprecipitation in a microfluidic reactor using water as carrier fluid: synthesis parameters optimization

3.2.1. Residence time

For the better control and the complete coprecipitation in small droplets formed in the microfluidic reactor it is necessary to optimize the residence time of the droplets. The residence time was controlled by the length of the capillaries at the exit of the microfluidic reactor, heated at the controlled temperature 65 °C. Three catalysts were prepared with different residence times (7, 30 and 140 s): $CZZ_{water\text{-}7s\text{-}1x\text{-}pH6}$, $CZZ_{water\text{-}30s\text{-}1x\text{-}pH6}$ and $CZZ_{water\text{-}140s\text{-}1x\text{-}pH6}$. Other parameters as reagents' flow rates, temperature and pH were not changed.

Table 3 Characterization of the CZZ catalysts with different synthesis residence times

Catalysts	Elementary analysis (wt %)#			$d_{app_{cat}}$ (g cm^{-3})	Crystallite size (nm)¤		S_{BET} (m^2 g^{-1})	S_{Cu^0} ($m_{Cu^0}^2$ g_{cat}^{-1})
	CuO (37.5)*	ZnO (41.0)*	ZrO_2 (21.5)*		CuO	ZnO		
$CZZ_{water\text{-}7s\text{-}1x\text{-}pH6}$	39	39	22	0.48	9	10	112	12.6
$CZZ_{water\text{-}30s\text{-}1x\text{-}pH6}$	40	38	22	0.42	10	11	99	9.4
$CZZ_{water\text{-}140s\text{-}1x\text{-}pH6}$	40	32	28	0.54	11	11	113	10.8

$CZZ_{a\text{-}b\text{-}c\text{-}d}$: a = vector fluid, b = residence time, c = flow multiplication, d = precipitation pH
 # determined by ICP-OES
*** theoretical values**
¤ determine by XRD with Debye-Scherrer equation

Table 3 summarizes the characterisation results of the catalysts synthesized different residence times. It can be seen that the copper mass content is stable regardless the residence time, but the mass content of ZnO decreases and the mass content of ZrO_2 increases when the residence time is longer. At the long residence time 140s it' s even more evident. So, the coprecipitation seems not complete during a long residence time in the $CZZ_{water\text{-}140s\text{-}1x\text{-}pH6}$ sample and a part of ZnO is missing being compensated by ZrO_2 content. Supposedly, the long residence time affects the gradient of salts concentration in each droplet and thus changing the media pH to a value which prevents the Zn cations precipitation. As the

composition of the materials at different residence time is not completely the same, it is difficult to compare the metallic copper surface between these three materials. The difference was considered as not important and it is similar to the trend of specific surface area values – higher the specific surface area, higher the measured metallic copper surface area.

The crystallites size of CuO for these three samples is varied slightly from 9 nm for $CZZ_{water\text{-}7s\text{-}1x\text{-}pH6}$, 10 nm for $CZZ_{water\text{-}30s\text{-}1x\text{-}pH6}$ and finally 11 nm for $CZZ_{water\text{-}140s\text{-}1x\text{-}pH6}$.

When the residence time is low, the metallic copper surface area reaches 12.6 $m_{Cu^{\circ}}^{2}$ g^{-1} for $CZZ_{water\text{-}7s\text{-}1x\text{-}pH6}$. When the residence time increases, the metallic copper surface area drops to 9.4 $m_{Cu^{\circ}}^{2}$ g^{-1} for $CZZ_{water\text{-}30s\text{-}1x\text{-}pH6}$ and to 10.8 $m_{Cu^{\circ}}^{2}$ g^{-1} for $CZZ_{water\text{-}140s\text{-}1x\text{-}pH6}$. The difference is not considerable and is similar to the trend of specific surface area values – higher the specific surface area, bigger the measured metallic copper surface area.

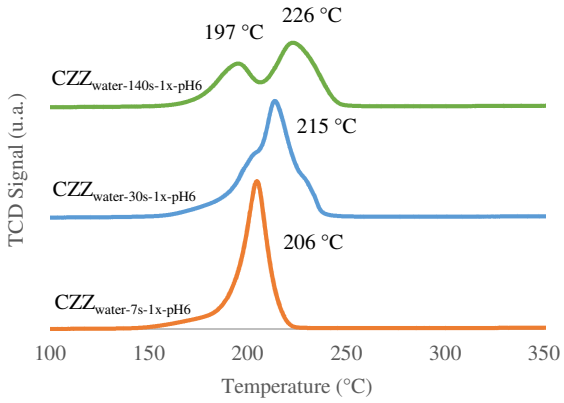

Figure 6 TPR-H_2 profiles of $CZZ_{water\text{-}7s\text{-}1x\text{-}pH6}$, $CZZ_{water\text{-}30s\text{-}1x\text{-}pH6}$ and $CZZ_{water\text{-}140s\text{-}1x\text{-}pH6}$ catalysts

Figure 6 presents the reduction profiles of the samples prepared with different residence times. The longer the residence time, the broader the reduction peaks. The shorter the residence time, the sharper and more symmetrical the reduction peak. The formation of different CuO species is thus evidenced. At short residence time only one kind of CuO species is formed that reduces at low reduction temperature (around 206 °C). Probably only one sort of CuO species is present, demonstrating quite weak CuO-support interactions. For a residence time of 30 s two shoulders appear before and after the main reduction peak at 215 °C. The long residence promotes quite heterogeneous CuO distribution over the support with two main different CuO species: at low temperature, around 200 °C (weak interaction with the support) and high temperature around 230 °C (stronger CuO-support interaction). The results indicate that a moderate residence time allows more homogeneous CuO-support interactions.

The three samples were tested as catalysts in CO_2 hydrogenation into methanol. The results at 280 °C are presented in *Table 4,* as well as the tests results of the samples described in the following sections. The temperature of 280°C was chosen according to the *Table 2*, as it was the optimal temperature for the methanol productivity. Conversions and selectivities obtained over each catalyst are very close. Regarding the MeOH productivity, the catalyst with an intermediate residence time of 30 s presented the best performance, reaching 1022 g_{MeOH} kg_{cat}^{-1} h^{-1} at 280 °C. *Table 4* shows the calculated TOF for the temperature of 280 °C. When the residence time is too short or too long (7 s or 140 s) the MeOH productivity, as well as TOF, are negatively impacted. For the better understanding of the influence of the residence time on materials properties and their catalytic activity it is necessary to study the coprecipitation kinetics in the microfluidic conditions in the confined channels, such study was never

performed for the Cu-, Zn- and Zr-containing materials and will be the subject of future investigations.

Table 4 Catalytic results at 280°C ,50 bar and 25,000 h^{-1} for CZZ catalysts with water as carrier fluid: effect of synthesis residence time, effect of reagents flow rate, effect of pH

Catalysts (mass[#])	Temperature (°C)	Conversion (%)		Selectivity (%)		MeOH productivity ($g\ kg_{cat}^{-1}\ h^{-1}$)	TOF ($10^3\ s^{-1}$)
		H_2	CO_2	MeOH	CO		
$CZZ_{water\text{-}7s\text{-}1x\text{-}pH6}$ (19.9 mg)	280	9.7	21.7	33	67	932	26.5
$CZZ_{water\text{-}30s\text{-}1x\text{-}pH6}$ (17.9 mg)	280	9.6	20.2	35	65	1022	38.9
$CZZ_{water\text{-}140s\text{-}1x\text{-}pH6}$ (22.7 mg)	280	10	20.7	36	64	825	27.4
$CZZ_{water\text{-}30s\text{-}2x\text{-}pH6}$ (28.2 mg)	280	11.3	24.6	32	68	704	21.7
$CZZ_{water\text{-}30s\text{-}4x\text{-}pH6}$ (29.7 mg)	280	11.4	24.5	33	67	688	23.2
$CZZ_{water\text{-}30s\text{-}1x\text{-}pH8}$ (15.6 mg)	280	9.9	21.4	33	67	1135	32.8
Thermodynamic simulation results	280	14.3	29.5	44	56	/	/

$CZZ_{a\text{-}b\text{-}c\text{-}d}$: a = vector fluid, b = residence time (s) , c = flow multiplication, d = precipitation pH
[#] calculated from the apparent density of each catalyst in keep constant GHSV

3.2.2. Reagents flow rates

The influence of the reagents flow rates during the synthesis was studied in this section. The reagents in question are the solution of metal nitrates and the solution of precipitating agent (sodium carbonate). Thus, it is expected that increasing the flowrates of the solutions will increase the amount of catalyst produced per unit of time. The carrier fluid flowrate was kept constant in all experiments at 1.7 mL min^{-1}. The flow rates for the ($CZZ_{water\text{-}30s\text{-}1x\text{-}pH6}$) material were fixed at 11.6 µL min^{-1} (metal nitrates) and 23.4 µL min^{-1} (precipitating agent) for the total reagent flow of 35 µL min^{-1}. Then the flowrates of the reagents were arbitrarily multiplied by 2 ($CZZ_{water\text{-}30s\text{-}2x\text{-}pH6}$) and by 4 ($CZZ_{water\text{-}30s\text{-}4x\text{-}pH6}$). The increase of reagents flow rate does not change the residence time which was kept constant at 30 s.
The main characteristics of the three catalysts discussed in this section are given in *Table 5*.

Table 5 Characterization of the CZZ catalysts with different reagents flow rates during the synthesis

Catalysts	Elementary analysis (wt %)[#]			$d_{app_{cat}}$ ($g\ cm^{-3}$)	Crystallite size (nm)[¤]		S_{BET} ($m^2\ g^{-1}$)	S_{Cu° ($m_{Cu^\circ}^2\ g_{Cat}^{-1}$)
	CuO (37.5)[*]	ZnO (41.0)[*]	ZrO_2 (21.5)[*]		CuO	ZnO		
$CZZ_{water\text{-}30s\text{-}1x\text{-}pH6}$	40	38	22	0.42	10	11	99	9.4
$CZZ_{water\text{-}30s\text{-}2x\text{-}pH6}$	45	30	25	0.66	10	11	99	11.6
$CZZ_{water\text{-}30s\text{-}4x\text{-}pH6}$	47	28	25	0.70	10	11	94	10.6

$CZZ_{a\text{-}b\text{-}c\text{-}d}$: a = vector fluid, b = residence time, c = flow multiplication, d = precipitation pH
 # determined by ICP-OES
*** theoretical values**
¤ determine by XRD with Debye-Scherrer equation

According to the ICP analysis, when the reagents flowrate is increased, the catalysts composition does no longer correspond to the expected one. The Cu content increases from 40 to 45 and 47 wt%, while the Zn content decreases from 38 to 30 and 28 wt%. This means that too high flowrates do not allow a good and complete coprecipitation of the zinc species. It is

probably due to the difference in kinetic rates of precipitation of different metallic species which affects the coprecipitation at very high flow rates. Consequently, all other parameters are also affected. The apparent density of the samples increases with the reagents' flowrate. The crystallites size and the specific surface area were not largely influenced. The metallic copper surface area is impacted, ranging from 9.4 $m_{Cu^0}^2$ g^{-1} for $CZZ_{water\text{-}30s\text{-}1x\text{-}pH6}$, to 11.6 $m_{Cu^0}^2$ g^{-1} for $CZZ_{water\text{-}30s\text{-}2x\text{-}pH6}$ and 10.6 $m_{Cu^0}^2$ g^{-1} for $CZZ_{water\text{-}30s\text{-}4x\text{-}pH6}$ probably due to the higher content of copper in the final material when the flowrate is increased.
The reduction profiles of $CZZ_{water\text{-}30s\text{-}1x\text{-}pH6}$, $CZZ_{water\text{-}30s\text{-}2x\text{-}pH6}$ and $CZZ_{water\text{-}30s\text{-}4x\text{-}pH6}$ catalysts are shown in *Figure 7*. When the reagents flow rate increases during the catalyst synthesis, the reduction zone is gradually split into two peaks, indicating heterogeneity of materials with the presence of two distinct CuO species.

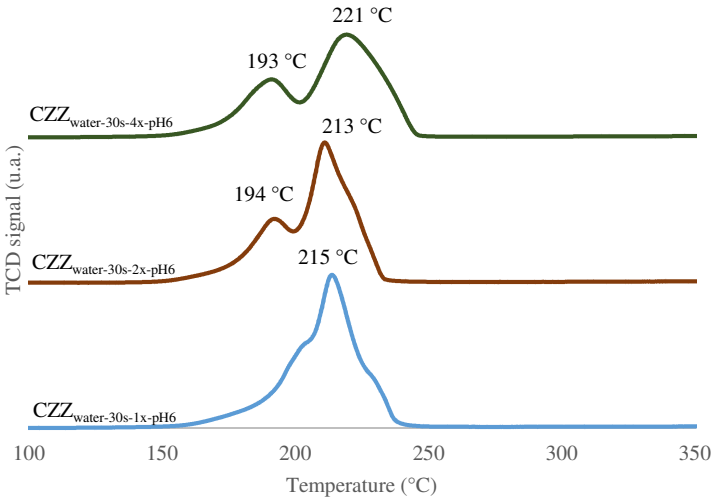

Figure 7 TPR-H_2 profiles of $CZZ_{water\text{-}30s\text{-}1x\text{-}pH6}$, $CZZ_{water\text{-}30s\text{-}2x\text{-}pH6}$ and $CZZ_{water\text{-}30s\text{-}4x\text{-}pH6}$ catalysts

Figure 8 shows scanning electron microscopy (SEM) images of $CZZ_{water\text{-}30s\text{-}1x\text{-}pH6}$, $CZZ_{water\text{-}30s\text{-}2x\text{-}pH6}$ and $CZZ_{water\text{-}30s\text{-}4x\text{-}pH6}$ catalysts. The morphology of the $CZZ_{water\text{-}30s\text{-}1x\text{-}pH6}$ catalyst has fine and porous layers, as already mentioned above. The morphology of the catalysts $CZZ_{water\text{-}30s\text{-}2x\text{-}pH6}$ and $CZZ_{water\text{-}30s\text{-}4x\text{-}pH6}$ is no longer in the form of fine sheets but it is rather granular and compact. By increasing the reagents flow rates, the morphology in layers is not formed. According to our previous work [45], the morphology of $CZZ_{water\text{-}30s\text{-}2x\text{-}pH6}$ and $CZZ_{water\text{-}30s\text{-}4x\text{-}pH6}$ is similar to the morphology obtained in the classical batch coprecipitation. However, the layered flower-like morphology was proved to be important for better CuO-support interactions and for the methanol productivity in the catalytic tests.

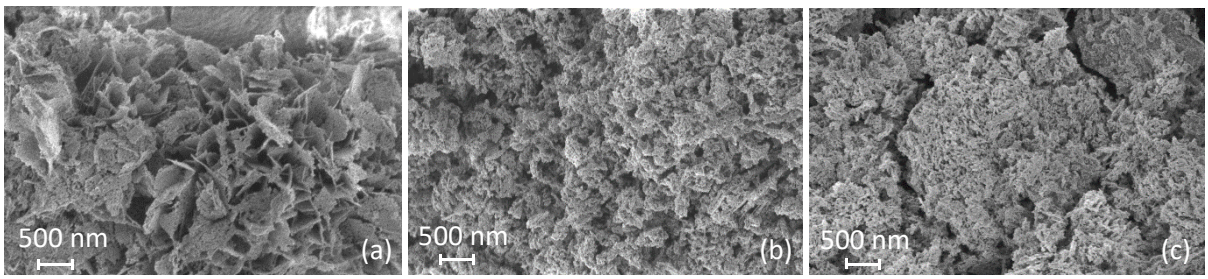

Figure 8 SEM images of (a) $CZZ_{water\text{-}30s\text{-}1x\text{-}pH6}$, (b) $CZZ_{water\text{-}30s\text{-}2x\text{-}pH6}$ and (c) $CZZ_{water\text{-}30s\text{-}4x\text{-}pH6}$

The catalytic results obtained over these three catalysts in CO_2 hydrogenation into methanol are presented in *Table 4*. If the reagents flow rate is kept low, the MeOH productivity could reach the record values 1022 g_{MeOH} kg_{cat}^{-1} h^{-1} for $CZZ_{water\text{-}30s\text{-}1x\text{-}pH6}$. The increase of the

reagents flow rates drastically decreases the methanol productivity 704 g_{MeOH} kg_{cat}^{-1} h^{-1} and 688 g_{MeOH} kg_{cat}^{-1} h^{-1} for $CZZ_{water\text{-}30s\text{-}2x\text{-}pH6}$ and $CZZ_{water\text{-}30s\text{-}4x\text{-}pH6}$, respectively. First of all, it is due to the different catalysts' compositions, lack of Zn and thus very heterogeneous CuO-support interaction. Secondly it is probably due to the compact morphology of the catalysts prepared with higher reagents flowrates. The values of methanol productivity in the case of $CZZ_{water\text{-}30s\text{-}2x\text{-}pH6}$ and $CZZ_{water\text{-}30s\text{-}4x\text{-}pH6}$ are close to that one obtained with the catalyst $CZZ_{66/34}$ prepared in batch coprecipitation (725 g_{MeOH} kg_{cat}^{-1} h^{-1} under the same conditions) [45].

3.2.3. Coprecipitation pH

Changing of the synthesis parameters as the droplets residence time and the reagents flow rate has evidenced that it is difficult to keep the coprecipitation complete with the respect of a desired composition. More often a part of zinc is missing. The precipitation of Zn^{2+} cations in form of carbonates or hydroxocarbonates is usually occurring at pH 5.1, at much higher pH than for the precipitation of Zr^{4+} (pH around 1) and Cu^{2+} (pH around 3). As the starting solution of metal nitrates is strongly acid (pH around 0.2), the gradient induced by its mixing with the basic solution of precipitating agent (pH around 9) is crucial for the precipitation of zinc cations as pH locally lower than 5 could affect their precipitation, even is the target mean pH is 6. In this section, the pH value of the coprecipitation media is studied in order to increase the possibility of complete coprecipitation. Two different coprecipitation pH were compared: 6 and 8, the respective samples, $CZZ_{water\text{-}30s\text{-}1x\text{-}pH6}$ and $CZZ_{water\text{-}30s\text{-}1x\text{-}pH8}$ are compared in this section.

Table 6 Characterization of the CZZ catalysts with different synthesis pH

Catalysts	Elementary analysis (wt %) #			$d_{app_{cat}}$ (g cm^{-3})	Crystallite size (nm)¤		S_{BET} (m^2 g^{-1})	S_{Cu^0} ($m_{Cu^0}^2$ g_{cat}^{-1})
	CuO (37.5)*	ZnO (41.0)*	ZrO_2 (21.5)*		CuO	ZnO		
$CZZ_{water\text{-}30s\text{-}1x\text{-}pH6}$	40	38	22	0.42	10	11	99	9.4
$CZZ_{water\text{-}30s\text{-}1x\text{-}pH8}$	40	38	22	0.37	10	10	99	12.4

$CZZ_{a\text{-}b\text{-}c\text{-}d}$: a = vector fluid, b = residence time, c = flow multiplication, d = precipitation pH
 # determined by ICP-OES
*** theoretical values**
¤ determine by XRD with Debye-Scherrer equation

The mass composition (*Table 6*) is identical for the two catalysts proving that a minimum pH of 6 is very important for the complete coprecipitation of all the components. A higher pH does not seem to affect the specific surface area (99 m^2 g^{-1} in both cases). The crystallite size of the CuO and ZnO are very close as well. These facts seems to be contradictory to the work of Lee *et al.* [36] on the characterization of the catalyst. Indeed, in their work it is indicated that the CuO and ZnO cristallite size increases and the surface area (S_{BET}) decreases when the coprecipitation pH increases. It is probably due to the difference in other synthesis parameters. Lee studied the batch coprecipitation synthesis and here we use a continuous synthesis in a microfluidic reactor. The apparent density is lower for the $CZZ_{water\text{-}30s\text{-}1x\text{-}pH8}$ comparing to $CZZ_{water\text{-}30s\text{-}1x\text{-}pH6}$ (0.37 and 0.42, respectively). The biggest difference was observed for the metallic copper surface area. Indeed, this surface is increased when pH of the synthesis media is increased, from 9.4 $m_{Cu^0}^2$ g^{-1} for the coprecipitation at pH 6 to 12.4 $m_{Cu^0}^2$ g^{-1} for the coprecipitation at pH 8. The H_2-consumption profiles of $CZZ_{water\text{-}30s\text{-}1x\text{-}pH6}$ and $CZZ_{water\text{-}30s\text{-}1x\text{-}pH8}$ catalysts are shown in *Figure 9.* The main reduction peak appears at the

temperature 215 °C for $CZZ_{water\text{-}30s\text{-}1x\text{-}pH6}$ and 208 °C for the $CZZ_{water\text{-}30s\text{-}1x\text{-}pH8}$. The profiles have similar shape. It can be noticed that the profile of $CZZ_{water\text{-}30s\text{-}1x\text{-}pH8}$ is slightly thinner and more homogeneous, without obvious shoulders and with only one zone of H_2 consumption, indicating a single kind of CuO species well interacting with the support in the catalysts. The increase of the synthesis media pH seems to slightly improve the homogeneity inside the catalyst.

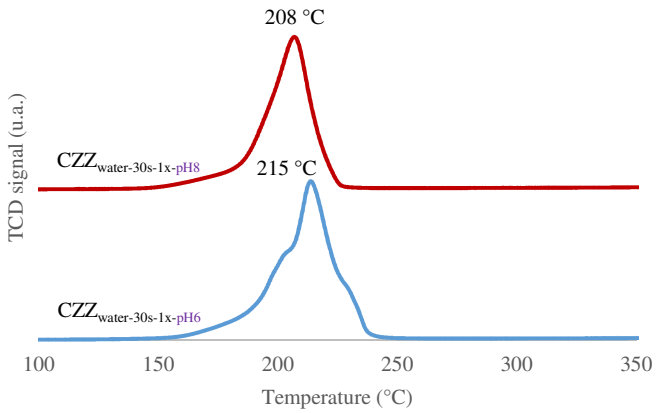

Figure 9 H_2 consumption of $CZZ_{water\text{-}30s\text{-}1x\text{-}pH6}$ and $CZZ_{water\text{-}30s\text{-}1x\text{-}pH8}$

Figure 10 represents the TEM images of the $CZZ_{water\text{-}30s\text{-}1x\text{-}pH8}$ catalyst. The TEM images of the $CZZ_{water\text{-}30s\text{-}1x\text{-}pH6}$ material are shown in *Figure 4(c)* and *4(d)*. The $CZZ_{water\text{-}30s\text{-}1x\text{-}pH8}$ catalyst is homogeneous in the same way as $CZZ_{water\text{-}30s\text{-}1x\text{-}pH6}$. Further analysis revealed the difference of the CuO crystallites size. The size of the crystals for the $CZZ_{water\text{-}30s\text{-}1x\text{-}pH8}$ catalyst observed in TEM is between 7 and 15 nm, which is smaller than the crystals size of the $CZZ_{water\text{-}30s\text{-}1x\text{-}pH6}$ (13-25 nm). These smaller crystals can explain the thinner TPR-H_2 profile and the improvement of the metallic copper surface area of $CZZ_{water\text{-}30s\text{-}1x\text{-}pH8}$.

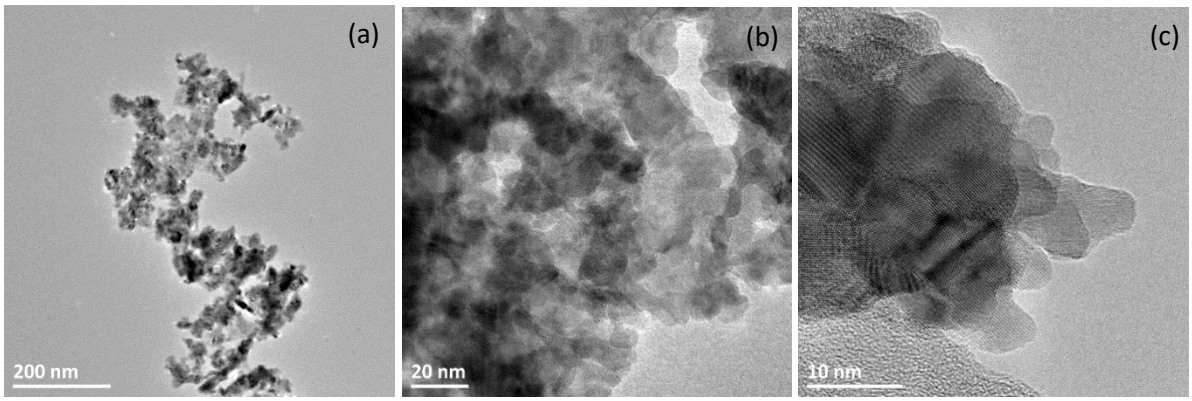

Figure 10 Bright field TEM images of $CZZ_{water\text{-}30s\text{-}1x\text{-}pH8}$

The catalytic results obtained over $CZZ_{water\text{-}30s\text{-}1x\text{-}pH6}$ and $CZZ_{water\text{-}30s\text{-}1x\text{-}pH8}$ in CO_2 hydrogenation into methanol are presented in *Table 4*. The $CZZ_{water\text{-}30s\text{-}1x\text{-}pH8}$ catalyst performs slightly higher CO_2 conversion than the $CZZ_{water\text{-}30s\text{-}1x\text{-}pH6}$ catalyst, over the entire temperature range. Indeed, with a higher coprecipitation pH, $CZZ_{water\text{-}30s\text{-}1x\text{-}pH8}$ is more homogeneous with smaller crystal size, thus higher Cu surface, compared to $CZZ_{water\text{-}30s\text{-}1x\text{-}pH6}$. In the same time, the MeOH productivity is always higher for $CZZ_{water\text{-}30s\text{-}1x\text{-}pH8}$, reaching the best productivity among all the catalysts, with 1135 $g_{MeOH}\ kg_{cat}^{-1}\ h^{-1}$ at 280 °C. The MeOH productivity in TOF values for the both materials are shown in *Table 4* as well. TOF calculations consider the metallic copper surface area, thus including more parameters than simple methanol

production per mass of catalyst. The TOF of the $CZZ_{water\text{-}30s\text{-}1x\text{-}pH6}$ appeared higher than TOF of $CZZ_{water\text{-}30s\text{-}1x\text{-}pH8}$ due to the difference in metallic copper surface areas of these two materials. It can be concluded that the increase of the coprecipitation media pH brings better CuO species distributions thanks to their smaller size thus creating a specific homogeneous mixture between catalyst components. As a result, the optimized catalyst $CZZ_{water\text{-}30s\text{-}1x\text{-}pH8}$ has the layered sheets morphology and the best catalytic properties.

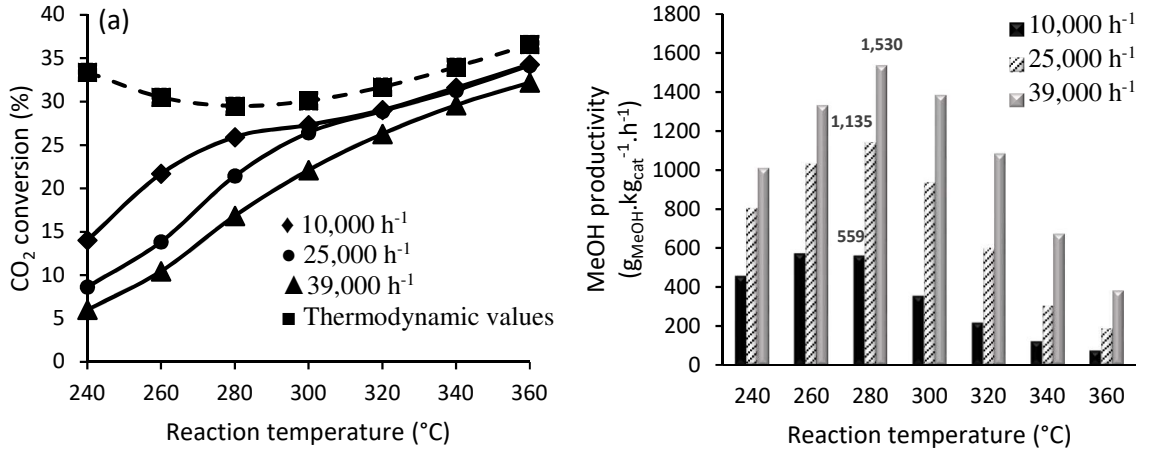

Figure 11 CO_2 conversion (a) and MeOH productivity (b) in the presence of $CZZ_{water\text{-}30s\text{-}1x\text{-}pH8}$ catalyst, at 50 bar and different GHSV

The choice of the high reagents flow was led by the thermodynamic limitations. The best catalytic results thus obtained for the $CZZ_{water\text{-}30s\text{-}1x\text{-}pH8}$ were questioned in different GHSV, in addition to 25,000 h^{-1} two more GHSV values were tested: 10,000 h^{-1} and 39,000 h^{-1}. *Figure 11* shows the results of these catalytic tests. Obviously, higher is the reagents GHSV further are the results from the thermodynamic equilibrium of the reaction. With the smallest tested GHSV equal to 10,000 h^{-1} the conversion of CO_2 reaches the thermodynamic equilibrium at already 280 °C; while the higher GHSV keeps the CO_2 conversion far from equilibrium even at high temperatures. It is worth to note, that the optimization of the synthesis parameters allowed to improve the productivity of methanol by 15%: previously obtained 486 $g_{MeOH}\,kg_{cat}^{-1}\,h^{-1}$ [37] *vs* 559 $g_{MeOH}\,kg_{cat}^{-1}\,h^{-1}$ (at 280 °C under 50 bar and a GHSV of 10,000 h^{-1}) (*Figure 11b*). The methanol productivity could be even further improved by increasing the GHSV: the methanol productivity 1530 $g_{MeOH}\,kg_{cat}^{-1}\,h^{-1}$ was obtained at 39,000 h^{-1}, 280°C, 50 bar.

Table 7 Comparison of the results with the recent literature

Catalysts	**H_2/CO_2**	**GHSV (h^{-1})**	**T (°C)**	**P (bar)**	**X_{CO2}-S_{MeOH} (%)**	**Productivity ($g_{MeOH}.kg_{Cat}^{-1}.h^{-1}$)**	**TOF ($10^3\ s^{-1}$)**
$CZZ_{water\text{-}30s\text{-}1x\text{-}pH6}$	3.9	25 000 10 000	280 280	50 50	16.5 – 47.0 25.4 – 32.5	1022 559	38.9 21.3
50Cu-Zn-Zr[49]	3.0	18 000	250	50	/ - /	665	5.2
50Cu-Zn-Al[50]	3.0	18 000	250	50	/ - 47.0	721	5.6
Cu/MgO/Al_2O_3-pH8[51]	2.8	2 000	250	20	3.6 – 31.0	8	-
ZrO_2/Cu-ZnO-350[52]	3.0		230	30	/ - /	499	-

The Table 7 presents a short list of the methanol productivity comparison in CO_2 hydrogenation reaction. The highest methanol productivity in similar conditions was obtained by Saito *et al*.[49,50] An interesting study was performed on $Cu/MgO/Al_2O_3$ catalysts with changing pH of the synthesis. It was shown that in the range of pH 5 – 11 the materials prepared at pH 8 are the most active, they were tested in CO_2 hydrogenation to methanol at 20 bar and achieved 8 $g_{MeOH}.kg_{Cat}^{-1}.h^{-1}$[51]. Another study of Stangeland *et al* on the coprecipitation-impregnation technics proves the great importance of the catalytic materials preparation, quite high methanol productivity 499 $g_{MeOH}.kg_{Cat}^{-1}.h^{-1}$ for ZrO_2 impregnated over Cu-ZnO catalyst was achieved at 30 bar[52]. The catalysts presented in this work prepared by the optimised coprecipitation in the microfluidic reactor are very competitive and in certain conditions are more efficient comparing to the other catalysts reported in the literature.

4. Conclusions

Cu-based catalysts with ZnO and ZrO_2 in the support were synthesized *via* a continuous coprecipitation in a microfluidic system, the theoretical composition of all the samples was kept at 37.5 wt% of CuO (corresponding to 30.0 wt% Cu^0), 41.0 wt% of ZnO and 21.5 wt% of ZrO_2. All the catalytic materials were characterized and tested as catalysts for the CO_2 hydrogenation into methanol at 50 bar in the range of 200-320 °C and different GHSV (10,000 h^{-1}, 25,000 h^{-1} and 39,000 h^{-1}) using high-throughput experiments. Several parameters specific to the synthesis in the microfluidic device have been modified in order to optimize the properties of the $CuO-ZnO-ZrO_2$ catalyst. The optimized microfluidic synthesis operation parameters were found: water as the carrier fluid, average residence time (30 s), the slow flow rate of the reagents during the synthesis (11.6 µL min^{-1} for metal nitrates and 23.4 µL min^{-1} for precipitating agent) and finally the increased pH of the coprecipitation synthesis (around pH 8).

Using water as the carrier fluid it was possible to prepare a catalyst more homogeneous and more efficient catalytically compared to the material prepared using silicon oil as the carrier fluid. The oil was discarded from the use as ecologically and economically not efficient (additional step of purification is needed). Too short or too long residence time of the droplets in the microfluidic reactor is not beneficial in terms of methanol productivity of the final catalyst due to uncompleted precipitation of all the catalysts components. The increase of the pH till 8 led to better homogeneity of the final catalyst. As a result, the record methanol productivity in comparison to the literature was achieved: 1135 g_{MeOH} kg_{cat}^{-1} h^{-1} at 25,000 h^{-1} at 50 bar at 280 °C for the $CuO-ZnO-ZrO_2$ catalyst ($CZZ_{water-30s-1x-pH8}$). The catalytic performances obtained in this work were largely improved by optimization of four parameters: carrier fluid nature, residence time, reagents flow rate and coprecipitation pH. In comparison to the best methanol productivities reported so far in the literature the here-reported results are very promising and can even be further optimized enlarging the studied parameters list, as it is currently under study.

Acknowledgements

The authors are grateful to Thierry Romero (ICPEES) and Corinne Bouillet (IPCMS) for the performance and the discussion on the results of TEM analyses. The authors acknowledge the ANR for the financial support (project DIGAS N°ANR-14-CE05-0012) with the $ValCO_2$ (Valorization of CO_2) for all the catalytic tests. The authors are thankful to Joëlle Thuriot Roukos (UCCS, Lille) for the ICP-OES analysis.

The REALCAT platform is benefiting from a governmental subvention administrated by the French National Research Agency (ANR) within the frame of the 'Future Investments' program (PIA), with the contractual reference 'ANR-11-EQPX-0037'. The Hauts-de-France region, the ERDF, Centrale Lille and Centrale Initiatives Foundation are warmly acknowledged for their financial contribution to the acquisition of the equipment of the REALCAT platform. Chevreul Institute (FR 2638), Ministère de l'Enseignement Supérieur, de la Recherche et de l'Innovation, Région Hauts-de-France and FEDER are acknowledged for supporting and funding partially this work.

References

[1] L.M. J. Rogelj, D. Shindell, K. Jiang, S. Fifita, P. Forster, V. Ginzburg, C. Handa, H. Kheshgi, S. Kobayashi, E. Kriegler, M.V.V. R. Séférian, M.V. Vilarino, K. Calvin, J.C. de Oliveira de Portugal Pereira, O. Edelenbosch, J. Emmerling, S. Fuss, T. Gasser, N. Gillett, C. He, E. Hertwich, L. Höglund-Isaksson, D. Huppmann, G. Luderer, A. Markandya, M. Meinshausen, D. McCollum, R. Millar, A. Popp, P. Purohit, K. Riahi, A. Ribes, H. Saunders, C. Schädel, C. Smith, P. Smith, E. Trutnevyte, Y. Xu, W. Zhou, K. Zickfeld, IPCC special report 2018, cap2, in: Global Warming of 1.5°C, (2018) 93–174. https://www.ipcc.ch/sr15/

[2] F. Shi, Y. Deng, T. SiMa, J. Peng, Y. Gu, B. Qiao, Alternatives to phosgene and carbon monoxide: Synthesis of symmetric urea derivatives with carbon dioxide in ionic liquids, Angew. Chemie - Int. Ed. 42 (2003) 3257–3260. doi:10.1002/anie.200351098.

[3] M. Aresta, A. Dibenedetto, A. Angelini, Converting "Exhaust" Carbon into "Working" Carbon, 1st ed., Elsevier Inc., 2014. doi:10.1016/B978-0-12-420221-4.00008-1.

[4] M. Taherimehr, P.P. Pescarmona, Green polycarbonates prepared by the copolymerization of CO_2 with epoxides, J. Appl. Polym. Sci. 131 (2014) 1–17. doi:10.1002/app.41141.

[5] A. Goeppert, M. Czaun, J. Jones, G.K.S. Prakash, G.A. Olah, Chem Soc Rev Recycling of carbon dioxide to methanol and derived products – closing the loop, 43 (2014) 7995-8048. doi:10.1039/c4cs00122b.

[6] G. A. Olah, A. Goeppert, G.K.S. Prakash, Chemical recycling of carbon dioxide to methanol and dimethyl ether: from greenhouse gas to renewable, environmentally carbon neutral fuels and synthetic hydrocarbons., J. Org. Chem. 74 (2009) 487–98. doi:10.1021/jo801260f.

[7] G.A. Olah, G.K.S. Prakash, A. Goeppert, Anthropogenic Chemical Carbon Cycle for a Sustainable Future, J. Am. Chem. Soc. 133 33 (2011) 12881–12898. doi:10.1021/ja202642y

[8] M. Alvarado, IHS Chemical Bulletin. The changing face of the global methanol industry, (2016) 10–11. https://cdn.ihs.com/www/pdf/IHS-Chemical-Bulletin-2016-Issue-3.pdf

[9] O.S. Santos, A.J.S. Mascarenhas, H.M.C. Andrade, N_2O-assisted methanol selective oxidation to formaldehyde on cobalt oxide catalysts derived from layered double hydroxides, Catal. Commun. 113 (2018) 32–35. doi:10.1016/j.catcom.2018.05.014.

[10] M. Xu, M. Xu, J. H. Lunsford, D. W. Goodman, A. Bhattacharyya, Synthesis of dimethyl ether (DME) from methanol over solid-acid catalysts, Appl. Catal. A 149 (1997) 289–301. doi:10.1016/S0926-860X(96)00275-X

[11] F.J. Keil, Methanol-to-hydrocarbons : process technology, Microporous and Microporous Materials 29 (1999) 49–66. doi:10.1016/S1387-1811(98)00320-5

[12] M. Aresta, A. Dibenedetto, A. Angelini, The changing paradigm in CO_2 utilization, J. CO_2 Util. 3–4 (2013) 65–73. doi:10.1016/j.jcou.2013.08.001.

[13] C.P. Nicolaides, C.J. Stotijn, E.R.A. Van Der Veen, M.S. Visser, Conversion of methanol and isobutanol to MTBE, Appl. Catal. A Gen. 103 (1993) 223–232. doi:10.1016/0926-860X(93)85053-R

[14] F. Lonis, V. Tola, G. Cau, Assessment of integrated energy systems for the production and use of renewable methanol by water electrolysis and CO_2 hydrogenation, Fuel. 285 (2021) 119160. https://doi.org/10.1016/j.fuel.2020.119160.

[15] A.C. Ince, C.O. Colpan, A. Hagen, M.F. Serincan, Modeling and simulation of Power-to-X systems: A review, Fuel. 304 (2021) 121354. https://doi.org/10.1016/j.fuel.2021.121354.

[16] D. Sheldon, Methanol Production – A Technical History, Johnson Matthey Technol. Rev. 61 (2017) 172–182.

doi:10.1595/205651317x695622.

[17] M. Kulawska, M. Madej-Lachowska, Copper/zinc catalysts in hydrogenation of carbon oxides, Chem. Process Eng. - Inz. Chem. i Proces. 34 (2013) 479–496. doi:10.2478/cpe-2013-0039.

[18] M. Pérez-Fortes, J.C. Schöneberger, A. Boulamanti, E. Tzimas, Methanol synthesis using captured CO_2 as raw material: Techno-economic and environmental assessment, Appl. Energy. 161 (2016) 718–732. doi:10.1016/j.apenergy.2015.07.067.

[19] M. Behrens, Coprecipitation: An excellent tool for the synthesis of supported metal catalysts – From the understanding of the well known recipes to new materials, Catal. Today. 246 (2015) 46–54. doi:10.1016/j.cattod.2014.07.050.

[20] S. Kühl, A. Tarasov, S. Zander, I. Kasatkin, M. Behrens, Cu-based catalyst resulting from a Cu,Zn,Al hydrotalcite-like compound: A microstructural, thermoanalytical, and in situ XAS study, Chem. - A Eur. J. 20 (2014) 3782–3792. doi:10.1002/chem.201302599.

[21] S.A. Kondrat, P.J. Smith, L. Lu, J.K. Bartley, S.H. Taylor, M.S. Spencer, G.J. Kelly, C.W. Park, C.J. Kiely, G.J. Hutchings, Preparation of a highly active ternary Cu-Zn-Al oxide methanol synthesis catalyst by supercritical CO_2 anti-solvent precipitation, Catal. Today. 317 (2018) 12-20. doi:10.1016/j.cattod.2018.03.046.

[22] H. Ren, C.-H. Xu, H.-Y. Zhao, Y.-X. Wang, J. Liu, J.-Y. Liu, Methanol synthesis from CO_2 hydrogenation over Cu/γ-Al_2O_3 catalysts modified by ZnO, ZrO_2 and MgO, J. Ind. Eng. Chem. 28 (2015) 261–267. doi:10.1016/j.jiec.2015.03.001.

[23] E.L. Kunkes, F. Studt, F. Abild-Pedersen, R. Schlögl, M. Behrens, Hydrogenation of CO_2 to methanol and CO on Cu/ZnO/Al_2O_3: Is there a common intermediate or not?, J. Catal. 328 (2015) 43–48. doi:10.1016/j.jcat.2014.12.016.

[24] C. Baltes, S. Vukojevic, F. Schuth, Correlations between synthesis, precursor, and catalyst structure and activity of a large set of CuO/ZnO/Al_2O_3 catalysts for methanol synthesis, J. Catal. 258 (2008) 334–344. doi:10.1016/j.jcat.2008.07.004.

[25] Y. Matsumura, H. Ishibe, Effect of zirconium oxide added to Cu/ZnO catalyst for steam reforming of methanol to hydrogen, J. Mol. Catal. A Chem. 345 (2011) 44–53. doi:10.1016/j.molcata.2011.05.017.

[26] F. Arena, K. Barbera, G. Italiano, G. Bonura, L. Spadaro, F. Frusteri, Synthesis, characterization and activity pattern of Cu–ZnO/ZrO_2 catalysts in the hydrogenation of carbon dioxide to methanol, J. Catal. 249 (2007) 185–194. doi:10.1016/j.jcat.2007.04.003.

[27] G. Bonura, M. Cordaro, C. Cannilla, F. Arena, F. Frusteri, The changing nature of the active site of Cu-Zn-Zr catalysts for the CO_2 hydrogenation reaction to methanol, Appl. Catal. B Environ. 152–153 (2014) 152–161. doi:10.1016/j.apcatb.2014.01.035.

[28] R.A. Koeppel, A. Baiker, Copper / zirconia catalysts for the synthesis of methanol from carbon dioxide Influence of preparation variables on structural and catalytic properties of catalysts, Appl. Catal. A Gen. 84 (1992) 77–102. doi:10.1016/0926-860X(92)80340-I

[29] H. Jeong, C.H. Cho, T.H. Kim, Effect of Zr and pH in the preparation of Cu/ZnO catalysts for the methanol synthesis by CO_2 hydrogenation, React. Kinet. Mech. Catal. 106 (2012) 435–443. doi:10.1007/s11144-012-0441-5.

[30] J.F. Portha, K. Parkhomenko, K. Kobl, A.C. Roger, S. Arab, J.M. Commenge, L. Falk, Kinetics of Methanol Synthesis from Carbon Dioxide Hydrogenation over Copper-Zinc Oxide Catalysts, Ind. Eng. Chem. Res. 56 (2017) 13133–13145. doi:10.1021/acs.iecr.7b01323.

[31] P. Gao, L. Zhang, S. Li, Z. Zhou, Y. Sun, Novel heterogeneous catalysts for CO_2 hydrogenation to liquid fuels, ACS Cent. Sci. 6 (2020) 1657–1670. doi:10.1021/acscentsci.0c00976.

[32] P. Gao, R. Xie, H. Wang, L. Zhong, L. Xia, Z. Zhang, W. Wei, Y. Sun, Cu/Zn/Al/Zr catalysts via phase-pure hydrotalcite-like compounds for methanol synthesis from carbon dioxide, J. CO_2 Util. 11 (2015) 41–48. doi:10.1016/j.jcou.2014.12.008.

[33] A. Le Valant, C. Comminges, C. Tisseraud, C. Canaff, L. Pinard, Y. Pouilloux, The Cu-ZnO synergy in methanol synthesis from CO_2, Part 1: Origin of active site explained by experimental studies and a sphere contact quantification model on Cu + ZnO mechanical mixtures, J. Catal. 324 (2015) 41–49. doi:10.1016/j.jcat.2015.01.021.

[34] L. Angelo, K. Kobl, L.M.M. Tejada, Y. Zimmermann, K. Parkhomenko, A.-C. Roger, Study of CuZnMOx oxides (M=Al, Zr, Ce, CeZr) for the catalytic hydrogenation of CO_2 into methanol, Comptes Rendus Chim. 18 (2015) 250–260. doi:10.1016/j.crci.2015.01.001.

[35] M. Behrens, D. Brennecke, F. Girgsdies, S. Kißner, A. Trunschke, N. Nasrudin, S. Zakaria, N.F. Idris, S.B.A. Hamid, B. Kniep, R. Fischer, W. Busser, M. Muhler, R. Schlögl, Understanding the complexity of a catalyst synthesis: Co-precipitation of mixed Cu,Zn,Al hydroxycarbonate precursors for Cu/ZnO/Al_2O_3 catalysts investigated by titration experiments, Appl. Catal. A Gen. 392 (2011) 93–102. doi:10.1016/j.apcata.2010.10.031.

[36] J.H. Lee, S.H. Lee, D.J. Moon, Preparation and characterization of Cu-based catalysts for methanol synthesis in MeOH-FPSO process, J. Nanosci. Nanotechnol. 13 (2013) 4398–4400. doi:10.1166/jnn.2013.7006.

[37] L. Angelo, M. Girleanu, O. Ersen, C. Serra, K. Parkhomenko, A.C. Roger, Catalyst synthesis by continuous coprecipitation under micro-fluidic conditions: Application to the preparation of catalysts for methanol synthesis from CO_2/H_2, Catal. Today. 270 (2015) 59–67. doi:10.1016/j.cattod.2015.09.028.

[38] X. Yao, Y. Zhang, L. Du, J. Liu, J. Yao, Review of the applications of microreactors, Renew. Sustain. Energy Rev. 47 (2015) 519–539. doi:10.1016/j.rser.2015.03.078.

[39] S. Kühl, M. Friedrich, M. Armbrüster, M. Behrens, Cu,Zn,Al layered double hydroxides as precursors for copper catalysts in methanol steam reforming - PH-controlled synthesis by microemulsion technique, J. Mater. Chem. 22 (2012) 9632–9638. doi:10.1039/c2jm16138a.

[40] A. Tanimu, S. Jaenicke, K. Alhooshani, Heterogeneous catalysis in continuous flow microreactors: A review of methods and applications, Chem. Eng. J. 327 (2017) 792–821. doi:10.1016/j.cej.2017.06.161.

[41] K.I. Sotowa, K. Irie, T. Fukumori, K. Kusakabe, S. Sugiyama, Droplet formation by the collision of two aqueous solutions in a microchannel and application to particle synthesis, Chem. Eng. Technol. 30 (2007) 383–388. doi:10.1002/ceat.200600345.

[42] S.Y. Teh, R. Lin, L.H. Hung, A.P. Lee, Droplet microfluidics, Lab Chip. 8 (2008) 198–220. doi:10.1039/b715524g.

[43] T. Fujitani, M. Saito, Y. Kanai, T. Kakumoto, T. Watanabe, J. Nakamura, T. Uchijima, The role of metal oxides in promoting a copper catalyst for methanol synthesis, Catal. Letters. 25 (1994) 271–276. doi:10.1007/BF00816307.

[44] T. Witoon, T. Numpilai, T. Phongamwong, W. Donphai, C. Boonyuen, C. Warakulwit, M. Chareonpanich, J. Limtrakul, Enhanced activity, selectivity and stability of a CuO-ZnO-ZrO_2 catalyst by adding graphene oxide for CO_2 hydrogenation to methanol, Chem. Eng. J. 334 (2018) 1781–1791. doi:10.1016/j.cej.2017.11.117.

[45] V. L'Hospital, L. Angelo, Y. Zimmermann, K. Parkhomenko, A.-C. Roger, Influence of the Zn/Zr ratio in the support of a copper-based catalyst for the synthesis of methanol from CO_2, Catal. Today. (2020) 183135. doi:10.1016/j.cattod.2020.05.018.

[46] K. Kobl, L. Angelo, Y. Zimmermann, S. Sall, K. Parkhomenko, A.-C. Roger, In situ infrared study of formate reactivity on water–gas shift and methanol synthesis catalysts, Comptes Rendus Chim. 18 (2015) 302–314. doi:10.1016/j.crci.2015.01.003.

[47] J.W. Evans, M.S. Wainwright, D.J. Young, On the determination of copper surface area by reaction with nitrous oxide, Appl. Catal. 7 (1983) 75–83. doi.org/10.1016/0166-9834(83)80239-5.

[48] L.E.Alexander, H.P. Kulg. X- Ray diffraction procedures: for polycrystalline and amorphous materials, (1974). ISBN: 978-0-471-49369-3

[49] M. Saito, T. Fujitani, M. Takeuchi, T. Watanabe, Development of copper/zinc oxide-based multicomponent catalysts for methanol synthesis from carbon dioxide and hydrogen, 138 (1996) 311–318.

[50] M. Saito, R&D activities in Japan on methanol synthesis from CO_2 and H_2, Catal. Surv. from Asia 2.2. 2 (1998) 175–184. https://doi.org/10.1023/A:1019082525994.

[51] V.D.B.C. Dasireddy, N.S. Štefančič, B. Likozar, Correlation between synthesis pH, structure and Cu/MgO/Al_2O_3 heterogeneous catalyst activity and selectivity in CO_2 hydrogenation to methanol, J. CO_2 Util. 28 (2018) 189–199. https://doi.org/10.1016/j.jcou.2018.09.002.

[52] K. Stangeland, H. H. Navarro, H. L. Huynh, W. M. Tucho, Z. Yu, Tuning the interfacial sites between copper and metal oxides (Zn, Zr, In)for CO_2 hydrogenation to methanol. Chem. Eng. Sci. 238, (2021), 116603. https://doi.org/10.1016/j.ces.2021.116603